



ELSEVIER

Available online at [www.sciencedirect.com](http://www.sciencedirect.com)

 ScienceDirect

Nuclear Physics B (Proc. Suppl.) 174 (2007) 7–10

**NUCLEAR PHYSICS B**  
**PROCEEDINGS**  
**SUPPLEMENTS**

[www.elsevierphysics.com](http://www.elsevierphysics.com)

# Jet production in the D0 experiment: measurements and data-to-Monte Carlo comparisons

Jeroen Hegeman <sup>a</sup> for the D0 Collaboration  
Nikhef Institute for Subatomic Physics Amsterdam  
University of Twente Enschede

<sup>a</sup>Nikhef

PO Box 41882

1009 DB Amsterdam, The Netherlands

E-mail: [jhegeman@fnal.gov](mailto:jhegeman@fnal.gov)

A preliminary measurement is presented of the inclusive jet production cross section in  $p\bar{p}$  collisions with the D0 detector using an integrated luminosity of  $\sim 800 \text{ pb}^{-1}$  of Tevatron RunII data. The cross section is studied as a function of jet  $p_T$  and rapidity and compared to perturbative QCD predictions in next-to-leading order including two-loop threshold corrections. Also presented is a preliminary measurement of  $Z/\gamma^*$ +jet production based on  $\sim 950 \text{ pb}^{-1}$ . A comparison to the SHERPA event generator shows excellent agreement for jet multiplicities and good agreement for the  $p_T$  spectra of the jets and the  $Z$  boson and for the inter-jet angular correlations.

## 1. Introduction

A broad range of physics can be studied in QCD jet production. Understanding high  $p_T$  jets can help constrain Parton Distribution Functions (PDFs) whereas soft jets allow one to study soft physics and hadronization. In addition, knowledge of multi-jet production is essential for understanding Standard Model backgrounds in the search for new physics.

## 2. Inclusive jet production cross section measurement

The cross section is measured in two central jet rapidity regions:  $|y_{\text{jet}}| < 0.4$  and  $0.4 < |y_{\text{jet}}| < 0.8$ .

### 2.1. Jet energy calibration

The measured jet energies are calibrated to the particle level using the expression

$$E_{\text{ptcl}} = \frac{E_{\text{cal}} - O}{R \cdot S} \quad (1)$$

which corrects for offset  $O$ , jet response  $R$  and detector showering effects  $S$ . The offset is determined from zero-bias events and corrects for

calorimeter noise, pile-up effects and the soft underlying event. The absolute response is determined by requiring  $p_T$  balance in photon+jet events. The photon energy scale is determined by calibrating the electromagnetic calorimeter on the  $Z \rightarrow e^+e^-$  peak and combining this with the relative electron-photon energy scale. Response dependence on detector pseudorapidity is determined using both photon+jet and dijet events. Parts of the particle shower in the calorimeter may escape the jet cone. A net correction for this showering effect is derived by measuring the energy density profile around a jet and subtracting the energy leaving the jet cone due to physics effects estimated from Monte Carlo.

### 2.2. Jet $p_T$ and rapidity resolutions

The jet  $p_T$  resolution is measured on a subsample of the full dataset used for the analysis by looking at the  $p_T$  imbalance in dijet events:

$$A = \frac{|p_{T,1} - p_{T,2}|}{p_{T,1} + p_{T,2}} \quad (2)$$

after corrections for soft radiation (resulting in additional jets below the reconstruction threshold) and particle level imbalances.

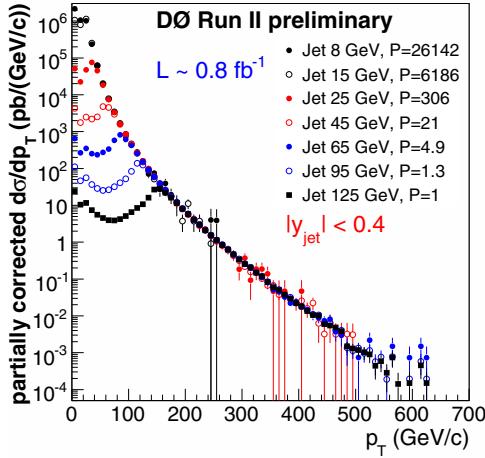


Figure 1. Partially corrected inclusive jet cross section in central rapidity, measured with different jet triggers at different  $p_T$  thresholds.

The jet  $p_T$  spectra are fitted iteratively with a four-parameter Ansatz function

$$f(N, \alpha, \beta, \gamma) = N(p_T/\text{GeV})^{-\alpha} \times \left(1 - \frac{2 \cosh(y_{\min}) p_T}{\sqrt{s}}\right)^\beta \exp(-\gamma p_T) \quad (3)$$

convoluted with the resolutions as determined from data. Here  $y_{\min}$  is the lower rapidity limit of the bin, and  $\sqrt{s}$  is the center-of-mass energy.

The ratio of fitted to original Ansatz function is used to unfold the data for resolution effects. Another method based on PYTHIA [1] events smeared with the data resolutions was used to cross-check this method and excellent agreement was obtained.

### 2.3. Results

Data from seven different jet triggers was selected for this measurement (see Fig. 1). The different trigger samples are matched using the relative trigger efficiencies and corrected for both jet identification and event selection efficiency.

To remove uncertainties due to the luminosity determination the results in Fig. 2 are normalized

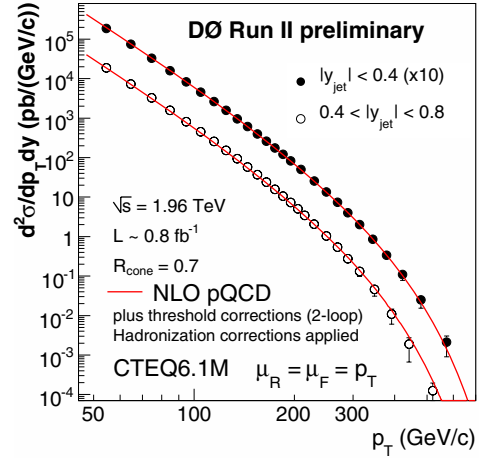


Figure 2. The inclusive jet cross section, measured in two regions of jet rapidity. Error bars show the total measurement uncertainty. The predictions from pQCD are corrected for hadronization effects and are overlaid on the data as lines.

to theory at  $p_T = 100$  GeV/c in the  $|y_{\text{jet}}| < 0.4$  bin. We note excellent agreement between the shape of the distribution in data and theory over the whole  $p_T$  region studied.

### 2.4. Comparison to theory prediction

The measured cross section is compared to the prediction from next-to-leading order (NLO) theory including two-loop accuracy threshold corrections [2]. The NLO calculations were performed with NLOJet++ [3] and FastNLO [4]. Figure 3 shows the ratio of data to theory prediction for both rapidity bins. Also shown are the uncertainty on the CTEQ6.1M [5] PDF (dashed lines) and the next-to-leading order theory prediction without threshold corrections (dash-dotted line). Note that the measurement is becoming precise enough to start constraining the PDFs at high  $p_T$ . Since the uncertainty on the PDFs is mainly due to the uncertainty on the gluon PDF at high momentum fraction  $x$ , this mainly constrains the gluon PDF.

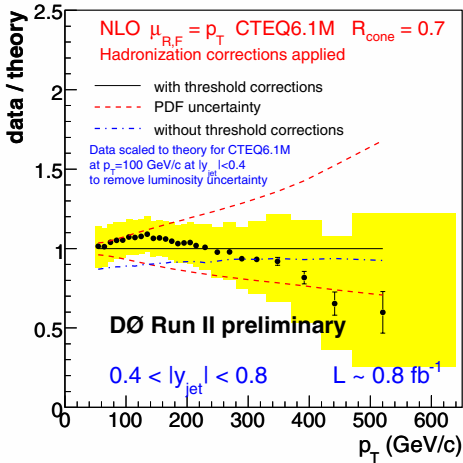
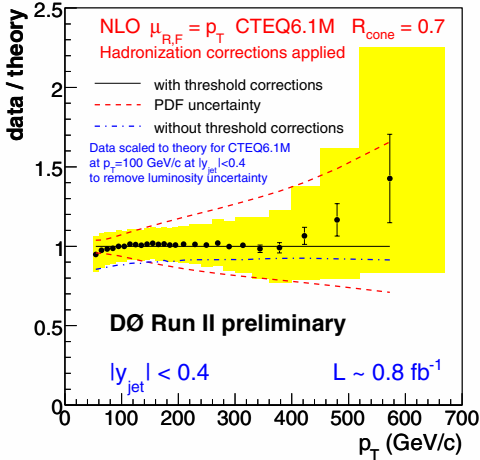


Figure 3. Inclusive jet cross section over theory, measured in two regions of jet rapidity. Error bars and band show statistical and systematic uncertainty, respectively.

### 3. Z+jets production at D0

The SHERPA [6] event generator implements the CKKW [7] algorithm. In contrast to traditional parton shower generators the CKKW algorithm generates  $2 \rightarrow N$  processes using tree-level diagrams only, applying phase space cuts to avoid divergences. The rest of the phase space is subsequently populated using a regular parton shower approach. The predictions of the SHERPA generator are compared to data for  $Z/\gamma^* + \text{jet}$  events in which  $Z/\gamma^* \rightarrow e^+e^-$ .

#### 3.1. Data and Monte Carlo samples

Data is selected using several single- and di-electron triggers. The Monte Carlo sample is generated with SHERPA version 1.0.6 using the CTEQ6L [5] PDFs and a  $k_T$  cutoff of  $(20 \text{ GeV})^2 / (1960 \text{ GeV})^2$  overlaid with zero-bias data. The Monte Carlo sample is normalized such that it contains the same total number of events as the data.

#### 3.2. Event selection

Only events containing both an electron and a positron with  $p_T > 25 \text{ GeV}/c$  and  $|\eta| < 2.5$  are used. In addition either the electron or the positron has to be central:  $|\eta| < 1.1$ . The jets in the Monte Carlo are smeared with resolutions functions from data.

#### 3.3. Results

As can be seen in Fig. 4, the predicted jet multiplicities from SHERPA agree well with data up to four jets. (Up to three jets were included in the matrix elements.) Also the  $Z$  boson  $p_T$  is very well described. The  $p_T$  spectrum of the leading jet is shown in Fig. 5(top) and shows very nice agreement with data. Note that the upward trend shown in the comparison of PYTHIA to data (Fig. 5(bottom)) is absent.

The  $p_T$  spectra of the second and third jet also match very well. The same holds for the distributions of  $\Delta\eta(\text{jet}, \text{jet})$  and inter-jet azimuthal angle  $\Delta\phi(\text{jet}, \text{jet})$ . Noteworthy is the fact that the SHERPA  $\Delta\phi$  distribution does not show an excess at  $\Delta\phi \sim \pi$ , while PYTHIA does [8].

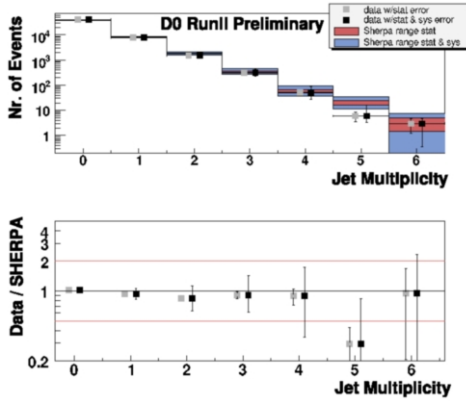
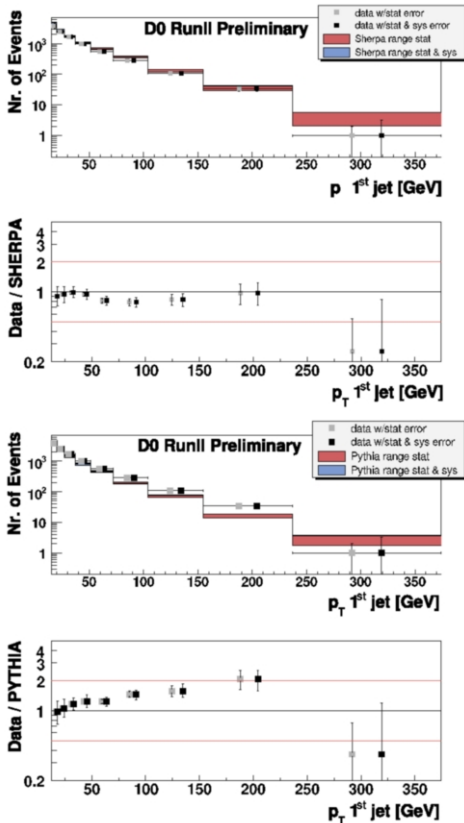


Figure 4. Jet multiplicities: data vs. SHERPA.

Figure 5. Leading jet  $p_T$ : data vs. SHERPA (top) and vs. PYTHIA (bottom)

#### 4. Conclusion

Preliminary results are presented on the inclusive jet cross section at D0. The results are in good agreement with next-to-leading order perturbative QCD. The measurement gains increasing sensitivity [9] to the gluon PDFs at high momentum transfers. This will be one of the leading uncertainties in searches beyond the standard model both at the Fermilab Tevatron Collider and at the CERN  $pp$  Collider (LHC).

Also presented is the first comparison between the SHERPA event generator and D0 data for  $Z/\gamma^* + \text{jets}$  events. The matrix element approach of SHERPA agrees very well with the data up to four jets, for the  $Z$  boson and jet  $p_T$  spectra as well as for the inter-jet  $\Delta\eta$  and  $\Delta\phi$  distributions.

#### REFERENCES

1. T. Sjöstrand *et al.*, Comp. Phys. Comm. **135**, 238 (2001).
2. N. Kidonakis, J.F. Owens, Phys. Rev. D **63**, 054019 (2001).
3. Z. Nagy, Phys. Rev. Lett. **88**, 122003 (2002); Z. Nagy, Phys. Rev. D **68**, 094002 (2003).
4. T. Kluge, K. Rabbertz and M. Wobisch, publication in preparation, <http://hepforge.cedar.ac.uk/fastnlo/>
5. J. Pumplin *et al.*, JHEP **0207**, 12 (2002); D. Stump *et al.*, JHEP **0310**, 046 (2003).
6. T. Gleisberg *et al.*, JHEP **0402** 056 (2004) [hep-ph/0311263].
7. S. Catani, F. Krauss, R. Kuhn and B. R. Webber, JHEP **0111** 063 (2001) [hep-ph/0109231]; F. Krauss, JHEP **0208** 015 (2002) [hep-ph/0205283].
8. V. Abazov *et al.* (D0 Collaboration), PRL **94** 221801 (2005) [hep-ex/0409040].
9. V. Abazov *et al.* (D0 Collaboration), PRL **82** 2451 (1999) [hep-ex/9807018].